Mon. Not. R. Astron. Soc. **000**, 000–000 (0000) Printed 8 January 2016 (MN LaTeX style file v2.2)

Exploring the systematical uncertainties of JLA supernova sample with redshift tomography method

Miao Li[1]⋆, Nan Li[1,2]†, Shuang Wang[1]‡ Lanjun Zhou[1,2]§

[1] *School of Astronomy and Space Science, Sun Yat-Sen University, Guangzhou 510275, P. R. China*
[2] *Kavli Institute for Theoretical Physics China, Chinese Academy of Sciences, Beijing 100190, P. R. China*

8 January 2016

ABSTRACT

In this work, by applying the redshift tomography method to Joint Light-curve Analysis (JLA) supernova sample, we explore the possible redshift-dependence of stretch-luminosity parameter α and color-luminosity parameter β. The basic idea is dividing the JLA sample into different redshift bins and assuming that α and β are piecewise constant; then constraining the ΛCDM model and checking the consistence of cosmology-fit results in each bin. We also adopt the same technique to explore which subsample of JLA plays a main role in causing systematical uncertainties. Using the full JLA data, we find that α is always consistent with a constant. In contrast, at high redshift β has a significant trend of decreasing, at $\sim 3.5\sigma$ confidence level (CL). Moreover, we find that low-z subsample favors a constant β; in contrast, SDSS and SNLS subsamples favor a decreasing β at 2σ and 3.3σ CL, respectively; in addition, HST subsample slightly slow down β's decreasing rate. These results imply that SNLS subsample plays a main role in causing β's evolution. Besides, by using a binned parameterization of β, we study the impacts of β's evolution on parameter estimation, and find that compared with a constant β, a varying β yields a larger best-fit value of fractional matter density Ω_{m0}, which slightly deviates from the best-fit result given by other cosmological observations. However, for both the varying β and the constant β cases, the 1σ regions of Ω_{m0} are still consistent with the result given by other observations.

Key words: cosmology: dark energy, observations, cosmological parameters, supernova

1 INTRODUCTION

Type Ia supernova (SN Ia) is a sub-category of cataclysmic variable stars that results from the violent explosion of a white dwarf star in a binary system Hillebrandt, & Niemeyer (2000). It can be used as standard candle to measure the expansion history of the universe Riess et al. (1998); Perlmutter et al. (1999), and it has become one of the most powerful tools to probe the nature of dark energy (DE) Frieman et al. (2008); Wang (2010); Li, Li, Wang, & Wang (2011, 2013); Weinberg et al. (2013). In recent years, several supernova (SN) datasets had been released, such as "SNLS" Astier et al. (2006), "Union" Kowalski et al (2008), "Constitution" Hicken et al. (2009a,b), "SDSS" Kessler et al. (2009), "Union2" Amanullah et al. (2010), "SNLS3" Conley et al. (2011) and "Union2.1" Suzuki et al. (2012). A latest SN sample is "Joint Light-curve Analysis" (JLA) dataset Betoule et al. (2014), which consists of 740 supernovae (SNe). JLA data includes 118 SNe at $0 < z < 0.1$ from several low-redshift samples (Hamuy et al. 1996; Riess et al. 1999; Jha et al. 2006; Contreras et al. 2010; Hicken et al. 2009a,b), 374 SNe at $0.03 < z < 0.4$ from the Sloan Digital Sky Survey (SDSS) SN search Holtaman et al. (2008), 239 SNe at $0.1 < z < 1.1$ from the Supernova Legacy Survey (SNLS) observations Guy et al. (2010) and 9 SNe at $0.8 < z < 1.3$ from Hubble Space Telescope (HST) Riess et al. (2007). It should be stress that, in the process of cosmology-fits, Betoule et al. treated two important quantities, stretch-luminosity parameter α and color-luminosity parameter β of SN Ia, as free model parameters Betoule et al. (2014). This procedure is same with the recipe of Conley et al. (2011).

As the sample size of SN Ia rapidly grows, the statistical uncertainties of SN Ia have been reduced effectively, and the systematical uncertainties have become more and more important. The main factors causing systematic uncertainties include the uncertainties in the photometric, the calibration, the identification of SN Ia, the selection bias, the host-galaxy extinction, the gravitational lensing and so on Hillebrandt, & Niemeyer (2000). In particular, one of the key factors is the potential evolution of SN, i.e., the possi-

⋆ mli@itp.ac.cn
† linan@itp.ac.cn
‡ wangshuang@mail.sysu.edu.cn (Corresponding author)
§ ljzhou@itp.ac.cn

bility of redshift-dependence of α and β. So far, there is no evidence for the evolution of α. But the redshift-dependence of β has been found for several SN datasets. For examples, by using the bin-by-bin method, Marriner et al. found the redshift-dependence of β for the SDSS data Marriner et al. (2011). Besides, by adopting a linear β, Mohlabeng and Ralston found the evolution of β at 7σ confidence level (CL) for the Union2.1 data Mohlabeng & Ralston (2013). In addition, one of the present authors had also done a series of research works about this issue. In Wang & Wang (2013a), we found that β deviates from a constant at 6σ CL for the SNLS3 data. Soon after, by studying various DE and modified gravity models with a linear β Wang, Li & Zhang (2014); Wang, et al. (2014); Wang, Wang & Zhang (2014); Wang, et al. (2015), we found that the evolution of β has significant effects on parameter estimation, and the introduction of a time-varying β can reduce the tension between SN Ia and other cosmological observations.

In a latest work Shariff et al. (2015), the discussion about time-varying β has been extended into the case of JLA data. By adopting two specific parameterizations of β, Shariff et al. found 4.6σ CL evidence for a significant drop in β at redshift $z = 0.66$ Shariff et al. (2015). It should be pointed out that, the results of Shariff et al. (2015) depend on two particular parameterizations of β. To extract more information about SN systematical uncertainties from JLA sample, it is necessary to revisit this issue with model independent method. In this work, we adopt the redshift tomography method, which has been widely used in the investigation of cosmology Marriner et al. (2011); Cai et al. (2014); Giannantonio et al (2015). The basic idea is dividing the SN data into different redshift bins and assuming that both α and β are piecewise constant. Then we constrain Λ-cold-dark-matter (ΛCDM) model and check the consistence of cosmology-fit results in each bin. In addition, it is very interesting to find out which subsample of JLA plays a main role in causing the systematical uncertainties of SN. As far as we know, this issue has not been studied in the past. Therefore, we also apply the same technique to various subsamples of JLA. Moreover, it is important to study the impacts of possible redshift-dependence of β on the parameter estimation. To do this, we adopt a binned parameterization of β in the analysis.

We describe our method in section 2, present our results in section 3, and summarize in section 4.

2 METHODOLOGY

In this section, we firstly introduce how to calculate the χ^2 function of JLA data. Then, we describe the details of redshift tomography method.

Theoretically, the distance modulus μ_{th} in a flat universe can be written as

$$\mu_{th} = 5\log_{10}\left[\frac{d_L(z_{hel}, z_{cmb})}{Mpc}\right] + 25, \tag{1}$$

where z_{cmb} and z_{hel} are the CMB restframe and heliocentric redshifts of SN. The luminosity distance d_L is given by

$$d_L(z_{hel}, z_{cmb}) = \frac{(1+z_{hel})c}{H_0}\int_0^{z_{cmb}}\frac{dz}{E(z)}, \tag{2}$$

where c is speed of light, H_0 is Hubble constant and $E(z) \equiv H(z)/H_0$ is the reduced Hubble parameter. For the case of ΛCDM model, $E(z)$ can be written as

$$E(z) = \sqrt{\Omega_{m0}(1+z)^3 + (1-\Omega_{m0})}. \tag{3}$$

Here Ω_{m0} is the present fractional matter density.

The observation of distance modulus μ_{obs} is given by a empirical linear relation:

$$\mu_{obs} = m_B^\star - M_B + \alpha \times X_1 - \beta \times \mathcal{C}, \tag{4}$$

where $m_B^\star$ is the observed peak magnitude in rest-frame B band, X_1 describes the time stretching of light-curve, $\mathcal{C}$ describes the supernova color at maximum brightness and M_B is the absolute B-band magnitude, which depends on the host galaxy properties Schlafly & Finkbeiner (2011); Johansson et al. (2013). Notice that M_B is related to the host stellar mass ($M_{stellar}$) by a simple step function Betoule et al. (2014)

$$M_B = \begin{cases} M_B^1 & \text{if} \quad M_{\text{stellar}} < 10^{10}\, M_\odot\,, \\ M_B^2 & \text{otherwise.} \end{cases} \tag{5}$$

Here $M_\odot$ is the mass of sun.

The χ^2 of JLA data can be calculated as

$$\chi^2 = \Delta\mu^T \cdot \mathbf{Cov}^{-1} \cdot \Delta\mu, \tag{6}$$

where $\Delta\mu \equiv \mu_{obs} - \mu_{th}$ is data vector and **Cov** is the total covariance matrix, which is given by

$$\mathbf{Cov} = \mathbf{D}_{\rm stat} + \mathbf{C}_{\rm stat} + \mathbf{C}_{\rm sys}. \tag{7}$$

Here the $\mathbf{D}_{\rm stat}$ is the diagonal part of the statistical uncertainty, which is given by Betoule et al. (2014),

$$\begin{aligned} \mathbf{D}_{\rm stat,ii} \;=\; & \left[\frac{5}{z_i \ln 10}\right]^2 \sigma^2_{z,i} + \sigma^2_{\rm int} + \sigma^2_{\rm lensing} + \sigma^2_{m_B,i} \\ & + \alpha^2\sigma^2_{X_1,i} + \beta^2\sigma^2_{\mathcal{C},i} + 2\alpha C_{m_B X_1,i} - 2\beta C_{m_B \mathcal{C},i} \\ & - 2\alpha\beta C_{X_1\mathcal{C},i}, \end{aligned} \tag{8}$$

where the first three terms account for the uncertainty in redshift due to the peculiar velocities, the intrinsic variation in SN magnitude and the variation of magnitudes caused by gravitational lensing. $\sigma^2_{m_B,i}$, $\sigma^2_{X_1,i}$, and $\sigma^2_{\mathcal{C},i}$ denote the uncertainties of m_B, X_1, and $\mathcal{C}$ for the i-th SN. In addition, $C_{m_B X_1,i}$, $C_{m_B\mathcal{C},i}$, and $C_{X_1\mathcal{C},i}$ are the covariances between m_B, X_1, and $\mathcal{C}$ for the i-th SN. Moreover, $\mathbf{C}_{\rm stat}$ and $\mathbf{C}_{\rm sys}$ are the statistical and the systematic covariance matrices, given by

$$\mathbf{C}_{\rm stat} + \mathbf{C}_{\rm sys} = V_0 + \alpha^2 V_a + \beta^2 V_b + 2\alpha V_{0a} - 2\beta V_{0b} - 2\alpha\beta V_{ab}, \tag{9}$$

where V_0, V_a, V_b, V_{0a}, V_{0b}, and V_{ab} are matrices given by the JLA group at the link: http://supernovae.in2p3.fr/sdss_snls_jla/ReadMe.html. For the detailed discussions about JLA SN sample, see Ref. Betoule et al. (2014).

As pointed out in Betoule et al. (2014), in the process of calculating χ^2, both the Hubble constant H_0 and the absolute B-band magnitude M_B are marginalized. In this work, we just follow the procedure of Betoule et al. (2014), and do not treat H_0 and M_B as free parameters. We refer the reader to Ref. Betoule et al. (2014), as well as the code of the JLA likelihood, for the details of calculation.

As mentioned above, our aim is exploring the possible evolution of SN with a model independent method. In this work, we adopt the redshift tomography method. The basic idea is dividing the SN sample into different redshift bins and assuming that both α and β are are piecewise constant. Then, by constraining the ΛCDM model, we check the consistence of cosmology-fit results given by the SN sample of each redshift bin. Moreover, to ensure that our results are insensitive to the details of redshift tomography, we evenly divide the JLA sample at redshift region [0,1] into 3 bins, 4 bins and 5 bins, respectively; then, we compare the fitting results obtained from these three cases. In this work we perform MCMC likelihood analysis using the "CosmoMC" package (Lewis & Bridle 2002).

3 RESULT

In this section, we mainly focus on the evolution behaviors of luminosity standardization parameters α and β. Firstly, we present the results given by full JLA sample; then, we present the results given by various subsamples of JLA.

In Fig 1, we plot the 1σ confidence regions of α given by the full JLA sample. The results of 3 bins, 4 bins and 5 bins are shown in the upper left panel, the upper right panel and the lower panel of Fig 1, respectively. For all the panels, it can be seen that the 1σ regions of α given by the full JLA sample (gray region) overlap with the results given by the SN samples of various bins at 1σ CL. So we can conclude that α is consistent with a constant. Since this conclusion holds true for all the cases of 3 bins, 4 bins and 5 bins, we can conclude that it is insensitive to details of redshift tomography. Moreover, this conclusion is consistent with the results of previous studies Marriner et al. (2011); Mohlabeng & Ralston (2013); Wang & Wang (2013a); Shariff et al. (2015).

In Fig 2, we plot the 1σ confidence regions of β given by the full JLA sample. The results of 3 bins, 4 bins and 5 bins are shown in the upper left panel, the upper right panel and the lower panel of Fig 2, respectively. It can be seen that, although β is consistent with a constant at low redshift, it has a significant trend of decreasing at high redshift. For the case of 3 bins, the 1σ upper bound of β in the last bin deviates from the results given by the full JLA sample at 3.5σ CL. For the case of 4 bins, the 1σ upper bound of β in the last bin deviates from the results given by the full JLA sample at 3.6σ CL. For the case of 5 bins, there is a hint for the evolution of β for the fourth bin; moreover, the 1σ upper bound of β in the last bin deviates from the results given by the full JLA sample at 3.6σ CL. These results indicate that β has a significant trend of decreasing, $\sim 3.5\sigma$ CL, at high redshift. This result is also insensitive to the details of redshift tomography. It must be stressed that, this conclusion is consistent with the results of some other SN samples Marriner et al. (2011); Mohlabeng & Ralston (2013), but is inconsistent with the results of the SNLS3 dataset, which indicates that β has a trend of increasing at high redshift Wang & Wang (2013a). The reason causing this tension is still unclear and deserves further studies.

As mentioned above, JLA dataset includes 118 SNe at $0 < z < 0.1$ from the low-z, 374 SNe at $0.03 < z < 0.4$ from the SDSS, 239 SNe at $0.1 < z < 1.1$ from the SNLS, and 9 SNe at $0.8 < z < 1.3$ from HST. It is important to find out which subsample plays a main role in causing the evolution of β. In this paper we only directly apply the redshift tomography method to the low-z, the SDSS, and the SNLS subsamples, because the HST subsample only contains 9 data points. To study the effects of HST subsample, we compare the results of β given by the JLA data removing HST with the results given by the full JLA sample.

In the Fig 3, making use of the redshift tomography method, we show the 1σ confidence regions of β given by each subsample. The results given by the low-z, the SDSS, and the SNLS subsamples are shown in the upper left panel, the upper right panel, and the lower panel of Fig 3, respectively. For simplicity, here we only consider the case of 4 bins. For the case of low-z, β is always consistent with a constant. For the case of SDSS, the 1σ upper bound of β in the last bin deviates from the results given by the full SDSS subsample at 2σ CL, showing that the SDSS subsample favors a decreasing β at high redshift. This conclusion is consistent with the results of Marriner et al. (2011). For the case of SNLS, the 1σ upper bounds of β in the third bin and the fourth bin deviate from the results of the full SNLS subsample at 1.6σ and 3.3σ CL, respectively. So compared with the case of SDSS, the SNLS subsample favors a time-varying β with a larger decreasing rate. It should be mentioned that, this conclusion is different from the results of the full SNLS3 sample Wang & Wang (2013a). This means that SNLS3 dataset may exists some unknown systematic uncertainties Betoule et al. (2014).

In Fig 4, we compare the 1σ confidence regions of β given by the JLA data removing HST (left panel) with the results given by the full JLA sample (right panel). We can see that the HST subsample only affect the evolution behavior of β at high redshift. For the case without HST, the 1σ upper bound of β in the last bin deviates from the results given by the full sample at 3.9σ CL. For the case of full JLA sample, the 1σ upper bound of β in the last bin deviates from the results given by the full JLA sample at 3.6σ CL. This indicates that HST subsample can slightly slow down the decreasing rate of β at high redshift.

According to the evolution behaviors of β given by various subsamples of JLA, we can conclude that the SNLS subsample plays a main role in causing the evolution of β.

Next, we discuss the impacts of a varying β on the parameter estimation. For simplicity, here we just consider the standard cosmological model: the ΛCDM model. As shown in Fig 2, β perfers a higher value at low redshift and a lower value at high redshift. So we assume that β is related to the redshift by a simple piecewise function

$$\beta(z) = \begin{cases} \beta_1 & 0 < z \leqslant 0.75\,, \\ \beta_2 & 0.75 < z \end{cases} \tag{10}$$

where β_1 and β_2 are two model parameters. In Fig 5, by using the full JLA sample only, we plot the 1D marginalized probability distributions of Ω_{m0} in the cases of constant β and varying $\beta(z)$. It can be seen that varying β yields a lager Ω_{m0} than the case of constant β: for the case of varying β, the best-fit value of Ω_{m0} is 0.329, while for the case of constant β, the best-fit value of Ω_{m0} is 0.297. Note that our result is consistent with the results of Shariff et al. (2015). To make a comparison, in Fig 5 we also plot the 1D marginalized probability distribution of Ω_{m0} given by a combination of the CMB Ade et al. (2015) [1] and the Baryon Acoustic Oscillations (BAO) Hemantha et al. (2014); Wang (2014) data. The best-fit value of Ω_{m0} given by CMB+BAO data is 0.292, which is more closer to the best-fit value of the constant β case. This result is different from the result of SNLS3 sample Wang, Li & Zhang (2014). However, Ω_{m0}'s result for the varying β case is still consistent with the result for the constant β case, as well as the result given by the CMB+BAO data, at 1σ CL.

4 SUMMARY

As the sample size of SN Ia rapidly grows, the statistical uncertainties of SN Ia have been reduced effectively, and the systematical uncertainties have become more and more important. One of the most important factors causing systematical uncertainties is the potential evolution of SN (i.e., the possibility of redshift-dependence of α and β), which has drawn a lot of attentions in recent years Marriner et al. (2011); Mohlabeng & Ralston (2013); Wang & Wang (2013a); Shariff et al. (2015).

In a latest work Shariff et al. (2015), using the JLA sample,

[1] In addition to Ade et al. (2015), there are some other CMB distance priors data, e.g. see Refs. Wang & Wang (2013b); Huang et al. (2015); Wang & Dai (2015).

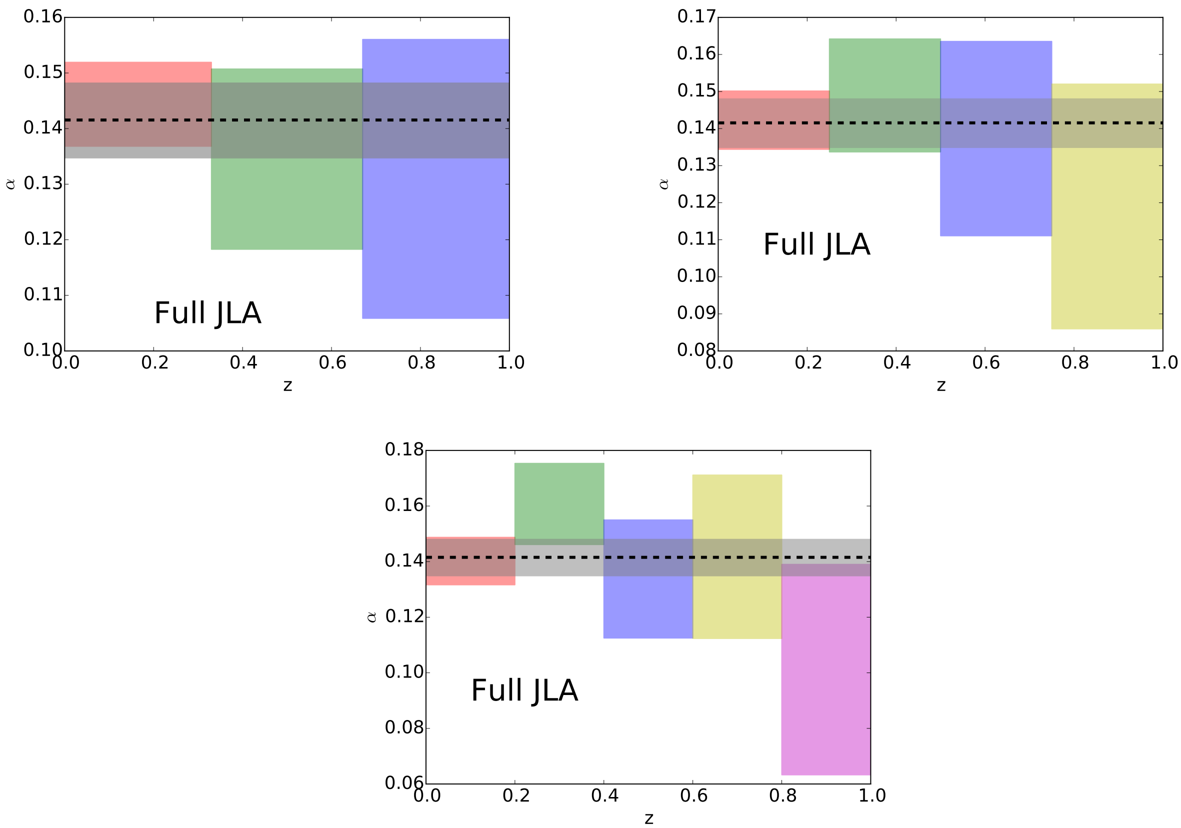

Figure 1. The 1σ confidence regions of stretch-luminosity parameter α given by the full JLA sample at redshift region [0,1]. The results of 3 bins, 4 bins and 5 bins are shown in the upper left panel, the upper right panel and the lower panel. The gray region and the gray dashed line denote the 1σ region and the best-fit result given by the full JLA data. The red, the green, the blue, the yellow and the purple regions correspond to the 1σ regions of the first, the second, the third, the fourth and the fifth bin, respectively.

Shariff et al. found 4.6σ CL evidence for a significant drop in β at redshift $z = 0.66$. Notice that the results of Shariff et al. (2015) depend on two particular parameterizations of β. To extract more information about SN systematical uncertainties from JLA sample, we revisit this issue with the redshift tomography method. To ensure that our results are insensitive to the details of redshift tomography, we take into account the cases of 3 bins, 4 bins and 5 bins, respectively. Then we constrain the ΛCDM model and check the consistence of cosmology-fit results in each bin. Moreover, in addition to the full JLA sample, we also apply the same technique to various subsamples of JLA, and then explore which subsample plays a more important role in causing the systematical uncertainties of SN. So far as we know, the effects of various JLA subsamples on β's evolution have not been studied in the past. Besides, the impacts of time-varying β is also studied.

In this work, using the full JLA sample, we find that the stretch-luminosity parameter α is always consistent with a constant (see Fig 1). In contrast, although β is still consistent with a constant at low redshift, it has a significant trend of decreasing, $\sim 3.5\sigma$ CL, at high redshift (see Fig 2). Since these conclusions hold true for all the cases of 3 bins, 4 bins and 5 bins, we can conclude that they are insensitive to the details of redshift tomography. It should be mentioned that, the evolution behaviors of β given by JLA sample are consistent with the results of some other SN samples Marriner et al. (2011); Mohlabeng & Ralston (2013), but are inconsistent with the results of SNLS3 dataset, which indicates that β has a trend of increasing at high redshift Wang & Wang (2013a). The reason causing this tension is still unclear and deserves further study.

Moreover, by studying the subsamples of JLA with the same technique, we find that low-z subsample favors a constant β; in contrast, both SDSS and SNLS subsamples favor a decreasing β at high redshift (see Fig 3). Besides, compared with SDSS subsample, SNLS subsample prefers a larger decreasing rate of β (see Fig 3). Notice that the results of β given by SDSS is consistent with the results of Marriner et al. (2011), but the results of β given by SNLS subsample is quite different from the results of Wang & Wang (2013a). This means that SNLS3 dataset may exists some unknown systematic uncertainties Betoule et al. (2014). In addition, although HST subsample only contains 9 data points, it can slightly slow down the decreasing rate of β at high redshift (see Fig 4). Based on the results of Figs 3 and 4, we can conclude that SNLS subsample plays a main role in causing the evolution of β.

In addition, we also study the impacts of possible redshift-dependence on parameter estimation using a binned parameterization of β. Making use of the full JLA sample only, we find that, compared with a constant β, a varying β yields a larger bestfit-fit value of Ω_{m0} , which is consistent with the conclusion of Shariff et al. (2015). We also compare the cosmological fitting result of JLA SN data with the result given by the CMB+BAO data. We find that the best-fit value of Ω_{m0} for the constant β case is more close to the result given by CMB+BAO data, which is different from the case of SNLS3 sample Wang, Li & Zhang (2014). However, Ω_{m0}'s

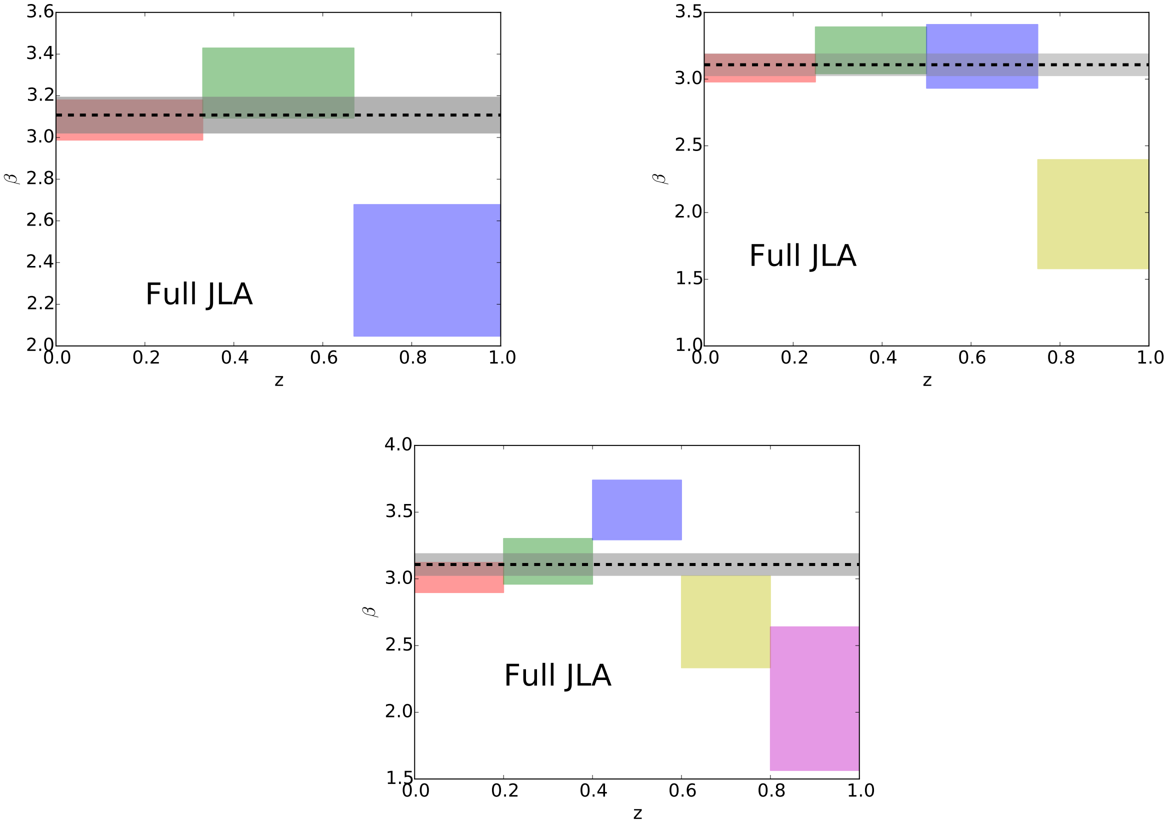

Figure 2. The 1σ confidence regions of color-luminosity parameter β given by JLA full sample at redshift region [0,1]. The results of 3 bins, 4 bins and 5 bins are shown in the upper left panel, the upper right panel and the lower panel. The gray region and the gray dashed line denote the 1σ region and the best-fit result given by the full JLA data. The red, the green, the blue, the yellow and the purple regions correspond to the 1σ regions of the first, the second, the third, the fourth and the fifth bin, respectively.

result for the varying β case is still consistent with the result for the constant β case, as well as the result given by other observations, at 1σ CL (see Fig 5).

In this paper, we only consider the simplest ΛCDM model. In addition to the ΛCDM model, many other DE models Li (2004); Chevallier & Polarski (2001); Linder (2003) are also favored by current cosmological observations. It is of interest to study the effects of varying β on parameter estimation in other dark energy models Zlatev et al. (1999); Caldwell (2002); Li (2004); Wang & Zhang (2008); Wang et al. (2008); Li et al. (2009a,b); Huang et al. (2009); Wang, Li & Li (2010, 2011). This will be done in future works.

Moreover, there are some other factors that can also cause the systematical uncertainties of SN, such as the evolution of intrinsic scatter σ_{int} Kim (2011); Marriner et al. (2011), the impacts of weak lensing Wang (2000); Wang, Chuang & Mukherjee (2012), and the impacts of different light-curve fitters Kessler et al. (2009); Bengochea (2011); Hu et al. (2015a,b,c). It is interesting to study the effects of these factors on cosmology-fits. We will investigate these issues in future.

ACKNOWLEDGMENTS

ML is supported by the National Natural Science Foundation of China (Grant No. 11275247, and Grant No. 11335012) and 985 grant at Sun Yat-Sen University. SW is supported by the National Natural Science Foundation of China under Grant No. 11405024 and the Fundamental Research Funds for the Central Universities under Grant No. N130305007.

REFERENCES

Ade P. A. R. et al., 2015, arXiv:1502.01589
Amanullah R. et al., 2010, ApJ, 716, 712
Astier P. et al., 2006, A&A, 447, 31
Bengochea G. R., 2011, Phys. Lett. B 696, 5
Betoule M. et al., 2014, A&A, 568, A22
Cai R.-G., Guo Z.-K., Tang B., 2014, Phys. Rev. D, 89, 123518
Caldwell R. R., 2002, Phys. Lett. B, 545, 23
Chevallier M., Polarski D., 2001, Int. J. Mod. Phys. D, 10, 213;
Conley A. et al., 2011, Astrophys. J. Suppl. 192, 1
Contreras C., et al. 2010, AJ, 139, 519
Frieman J. A., Turner S. M., Huterer D., 2008 Ann. Rev. Astron. Astrophys. 46, 385
Giannantonio T. et al., 2015 arXiv:1507.05551
Guy J. et al., 2010, A&A, 523, 7
Hamuy M. et al., 1996, AJ, 112, 2408
Hemantha M. D. P., Wang Y., Chuang C.-H., 2014, MNRAS, 445, 3737

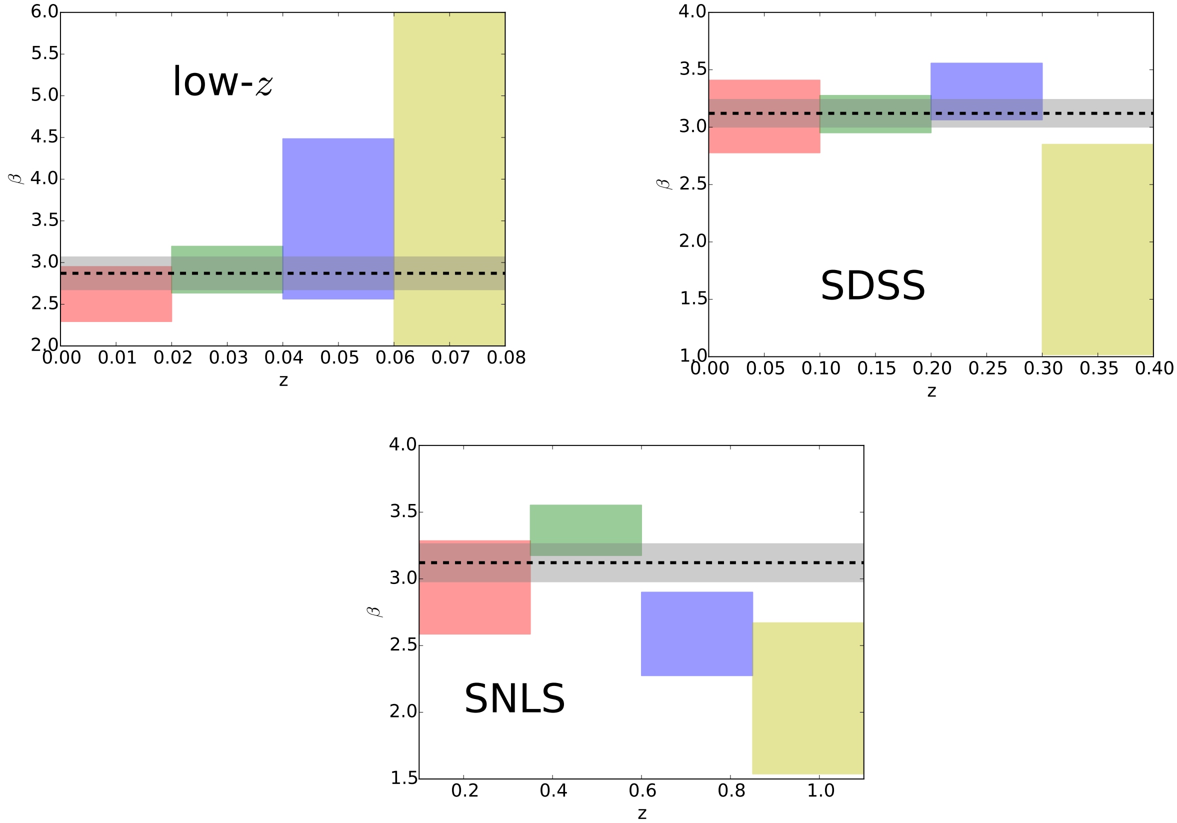

Figure 3. The 1σ confidence regions of β given by the three subsamples: low-z (upper left panel), SDSS (upper right panel) and SNLS (lower panel). The gray region and the gray dashed line are the 1σ region and the best-fit result given by the full low-z, the full SDSS and the full SNLS subsample, respectively. The red, the green, the blue and the yellow regions correspond to the 1σ regions of the first, the second, the third and the fourth bin, respectively.

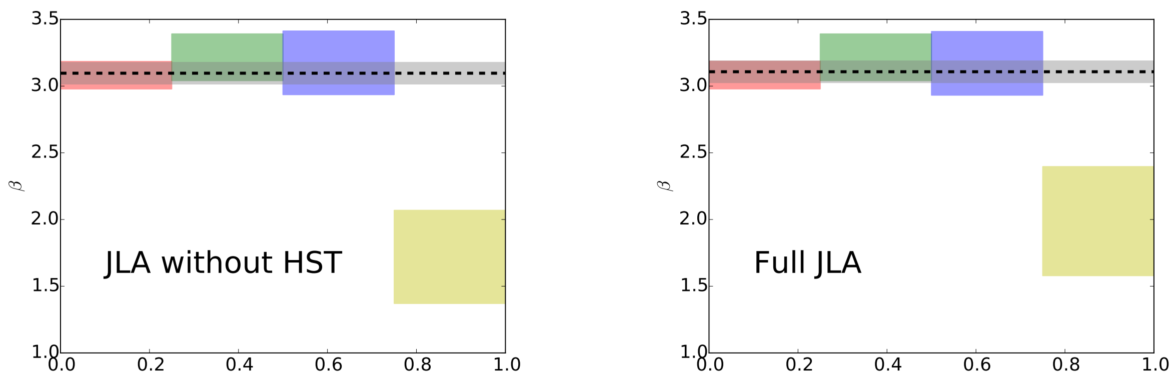

Figure 4. The 1σ confidence regions of β given by the JLA sample removing HST (left panel) and the full JLA sample (right panel) at redshift region [0,1]. The gray regions and the gray dashed lines denote the 1σ regions and the best-fit results given by the full samples, respectively. The red, the green, the blue and the yellow regions correspond to the 1σ regions of the first, the second, the third, and the fourth bin, respectively.

Hicken M., Wood-Vasey W. M., Blondin S., Challis P., Jha S., Kelly P. L., Rest A., Kirshner R. P., 2009, ApJ., 700, 1097;

Hicken M. et al., 2009, ApJ., 700, 331

Hillebrandt W., Niemeyer J. C., 2000, Ann. Rev. Astron. Astrophys. 38, 191

Holtzman J., et al. 2008, AJ, 136, 2306

Huang Q. G., Li M., Li X.-D., & Wang S., 2009, Phys. Rev. D, 80, 083515

Huang Q.-G., Wang S., Wang K., 2015, JCAP, 12, 022

Hu Y.-Z., Li M., Li N., Wang S., 2015, arXiv:1501.06962

Hu Y.-Z., Li M., Li N., Wang S., 2015, arXiv:1506.08274

Hu Y.-Z., Li M., Li N., Wang S., 2015, arXiv:1509.03461

Jha S. et al., 2006, AJ, 131, 527

Johansson J. et al., 2013, MNRAS, 435, 1680

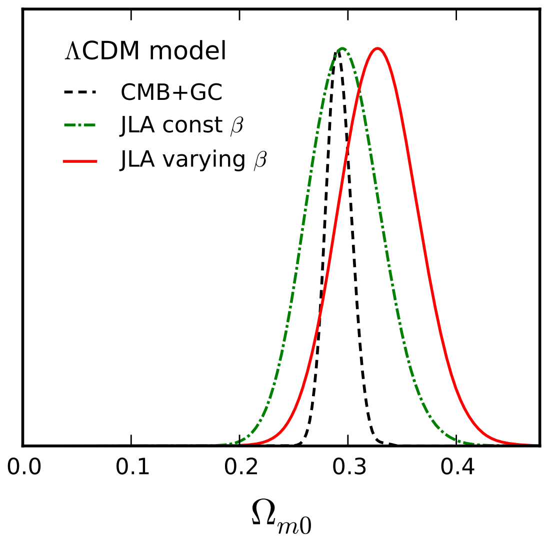

Figure 5. The 1D marginalized probability distributions of Ω_{m0} given by the full JLA sample for the ΛCDM model. Both the results of constant β (green dash-dotted line) and varying β (red solid line) cases are presented. The corresponding results given by the CMB+BAO data (black dashed line) are also shown for comparison.

Kessler R., et al., 2009, ApJS., 185, 32
Kim A., 2011, Publ. Astron. Soc. Pac., 123, 230
Kowalski M., et al., 2008, ApJ., 686, 749
Lewis A., Bridle S., 2002, Phys. Rev. D, 66, 103511
Li M., 2004, Phys. Lett. B, 603 1
Li M., Li X.-D., Wang S., Wang Y., Zhang X., 2009a, JCAP, 12, 014
Li M., Li X.-D., Wang S., Zhang X., 2009b, JCAP, 06, 036
Li M., Li X.-D., Wang S., Wang Y., 2011, Commun. Theor. Phys. 56, 525
Li M., Li X.-D., Wang S., Wang Y., 2013, Frontiers of Physics 8, 828
Linder E. V., 2003, Phys. Rev. Lett. 90, 091301.
Marriner J. et al., 2011, ApJ. 740, 72
Mohlabeng G., Ralston J., 2013, MNRAS, 439, L16
Perlmutter S. et al., 1999, ApJ, 517, 565
Riess A. G. et al., 1998, AJ, 116, 1009
Riess A. G. et al., 1999, AJ, 117, 707
Riess A. G. et al., 2007, ApJ. 659, 98
Schlafly E. F., Finkbeiner D. P., 2011, ApJ. 737, 103
Shariff H., Jiao X., Trotta R., Dyk D. A. v., arXiv:1510.05954
Suzuki N. et al., 2012, ApJ, 746, 85
Wang S., Geng J.-J., Hu Y.-L., Zhang X., 2015, Sci. China Phys. Mech. Astron. 58, 019801
Wang S., Li X.-D., Li M., 2010, Phys. Rev. D, 82, 103006
Wang S., Li X.-D., Li M., 2011, Phys. Rev. D, 83, 023010
Wang S., Li Y.-H., Zhang X., 2014, Phys. Rev. D, 89, 063524
Wang S., Wang Y., 2013, Phys. Rev. D, 88, 043511
Wang S., Wang Y.-Z., Geng J.-J., Zhang X., 2014, Eur. Phys. J. C 74, 3148
Wang S., Wang Y.-Z., Zhang X., 2014, Commun. Theor. Phys. 62, 927
Wang, S. & Zhang, Y. 2008, Phys. Lett. B, 669, 201
Wang S., Zhang Y., Xia T.-Y., 2008, JCAP, 10, 037
Wang Y., 2000, ApJ, 536, 531.
Wang Y., *Dark Energy*, Wiley-VCH, 2010, New York, (2010)
Wang Y., 2014, MNRAS, 443, 2950
Wang Y., Chuang C. H., Mukherjee P., 2012, Phys. Rev. D, 85, 023517
Wang Y., & Dai M. arXiv:1509.02198
Wang Y., & Wang S. 2013, Phys. Rev. D, 88, 043522
Weinberg D. H., Mortonson M. J., Eisenstein D.J. et al. 2013, Physics Reports, 530, 87
Zlatev I., Wang L. Steinhardt P.J. 1999, Phys. Rev. Lett., 82, 896